

# The use of a convective heat flow model in road designs for Northern regions

Lukas U. Arenson

University of Alberta, Department of Civil and Environmental Engineering

David C. Sego

University of Alberta, Department of Civil and Environmental Engineering

Greg Newman

GEO-SLOPE International Ltd.

**ABSTRACT** Roads and highways in northern environments are exposed to harsh climatic conditions. In particular, changes in temperature of several tens of degrees centigrade between the seasons, and substantial precipitation as well as permafrost conditions are common. These environmental conditions result in significant damages to the infrastructure that requires extensive maintenance. Road damage is directly related to problems associated with the foundation, frequently resulting in differential settlements. Significant increase in these problems is expected as a result of changing climate, thus reducing the expected service life of various roads in arctic regions. The highway system within the permafrost region is extremely vulnerable to these climate changes because the mechanical property of the soil changes dramatically with temperature increases and as ice within the frozen soil thaws. This paper presents a numerical investigation of a novel approach for an improvement of road foundations resulting from convective heat flow. The proposed foundation is capable of compensating for some of the expected warming of the permafrost by storing and maintaining the cold winter temperatures through the summer months. The numerical model demonstrated the importance of considering convective heat flows to optimize the design of the foundation with a focus on minimizing the effect of climate warming.

**KEY WORDS** *Permafrost, Embankment design, Air convection, Numerical modeling*

## Introduction

Infrastructure in northern environment experiences severe climatic conditions, have to be addressed during the design and construction. Seasonal temperature changes may be in the order of several tens of degree centigrade, significant amount of precipitation in form of snow and rain has to be expected, as well as permafrost conditions have to be tackled.

According to the Geological Survey of Canada, permafrost underlies more than 50% of the ground surface of Canada. Three divisions of permafrost can be distinguished, which are continuous permafrost, widespread discontinuous permafrost and sporadic permafrost. In northern Canada, permafrost thickness may exceed 500m, but permafrost can also occur in localized areas, where it is found in small isolated lenses in peat and affects only minor parts of the land area (Smith and Burgess, 1998; Smith and Burgess, 1999).

Significant damages to engineered structures exposed to such ground and climatic conditions require extensive maintenance. These damages are directly related to problems associated with the foundation, often resulting in differential settlements because of heterogeneous thermal ground and loading situations. In consequence, maintenance costs are likely to increase relative to those costs at present (Instanes, 2005).

It is expected that changing climate conditions, such as warmer temperatures and increased precipitations, will

increase these problems in the future and reduce the expected service life of various roads in arctic regions. In particular regions of warm and discontinuous permafrost are extremely vulnerable to these climate changes because the strength and deformation properties of the soil changes dramatically with even small temperature increases and as ice within the frozen soil thaws (eg. Andersland and Ladanyi, 2004).

In order to reduce the impact of future warming on embankments, innovative designs are required. Several laboratory and field studies have shown that some sort of ventilation of the embankment can reduce the warming of the ground (Goering and Kumar, 1996; Wu et al., 2002; Lai et al., 2004a; Lai et al., 2004b; Cheng, 2005; Liu and Lai, 2005; Yu et al., 2005; Ma et al., 2006). The insulating effect of the embankment ventilation with air is a result of a combination of the low air thermal conductivity and convective air fluxes. This main principle can not only be used for the design of new embankments and foundations, but also to improve current designs, expanding their service life, and reducing the cost of maintenance.

This paper presents an improved numerical model based on finite elements that incorporates air convection and was used for an initial numerical simulation of embankment improvements. Using constructed high air permeable shoulders significantly reduces the risk of permafrost thaw underneath the embankment toe. However, further analysis including more detailed sensitivity analysis as well as field investigations are required to improve the numerical model,

refine necessary soil properties and boundary conditions, and determine optimal embankment designs for various locations and geometry.

## Air Convection

Air has a very low thermal conductivity (2.25 kJ/(day·m·K)) and therefore it is a very good thermal insulator. However, changes in the thermal regime due to air convection, ie. heat energy transfer associated with air movements, can be significant and change the ground temperatures. In addition, the density of the air changes with temperature (Fig. 1). This change in air density enhances a gravity driven air movement as soon as a thermal gradient is present. Cold air, which is heavier than warm air, will sink and warm air will rise accordingly. Such air movements have an influence on the ground thermal regime in particular for soils with high air permeability, such as dry gravel, and blocky soil layers.

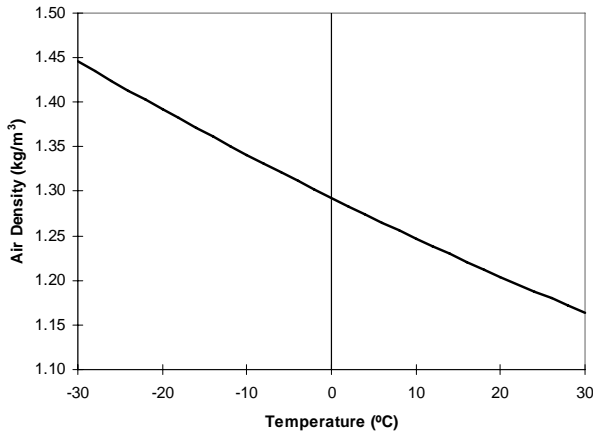


Figure 1. Change in air density as a function of temperature.

Kane *et al.* (2001) show that the assertion that pure conductive heat transfer always dominates in cold climates is not correct and that non-conductive heat transfer by water and water-vapor are significant, if not dominant under certain conditions. The effect of air convective heat fluxes on the temperatures beneath an embankment was shown amongst others by Goering and Kumar (1996) using an unsteady finite element model. Their numerical model showed that the winter-time natural convection occurring in high-permeability embankment reduces the average annual temperatures of the foundation by approximately 5°C. Their numerical simulations were later confirmed with data from a field investigations (Saboundjian and Goering, 2003).

## Numerical Code

Convective air fluxes have recently been incorporated into the GeoStudio software package (GeoStudio 2006). The program simultaneously solves air and water flow within unsaturated soils. SEEP/W has been modified to solve for compressible air flow in response to hydraulic, phematic and thermal boundary conditions. The SEEP/W air flow module can consider changes in air density due to temperature and, in response, TEMP/W can be used to compute the convective heat transfer associated with both moving water and moving air.

## Conservation of mass (general form)

For compressible flow the general form of the conservation of mass equation is:

$$\frac{\partial(\rho_f \theta_f)}{\partial t} = \frac{\partial}{\partial y} \left[ -(\rho_f K_f) \frac{\partial H_f}{\partial y} \right] + \rho_f Q_f$$

Where the subscript  $f$  is for any fluid and  $H$  is the total energy potential comprised of both pressure and elevation potentials, and expressed in terms of an equivalent column of water as:

$$H_f = \left( \frac{P_f}{\gamma_w} + \frac{\rho_f}{\rho_w} y \right)$$

## Water conservation of mass

The left side of the general equation can be expanded using the chain rule:

$$\frac{\partial(\rho_w \theta_w)}{\partial t} = \theta_w \frac{\partial \rho_w}{\partial t} + \rho_w \frac{\partial \theta_w}{\partial t}$$

The right hand side in the general equation can also be expanded using the chain rule:

$$\frac{\partial}{\partial y} \left[ (\rho_w K_w) \frac{\partial H_w}{\partial y} \right] = K_w \frac{\partial H_w}{\partial y} \frac{\partial \rho_w}{\partial y} + \rho_w \frac{\partial}{\partial y} \left[ K_w \frac{\partial H_w}{\partial y} \right]$$

Since water is assumed incompressible, the time derivative and spatial derivative of density terms in the above two equations are zero. The remaining density variable can be cancelled from all term so that the mass balance equation for water becomes a volume balance equation:

$$\frac{\partial(\theta_w)}{\partial t} = \frac{\partial}{\partial y} \left[ K_w \frac{\partial(H_w)}{\partial y} \right] + Q_w$$

Introducing matric suction as the difference in capillary pressure between air and water:

$$\psi = -(P_a - P_w) = [(\gamma_w H_w - gy) - P_a]$$

The left side of the water flow equation can be changed to be the time derivative of total head by using the slope of the water content versus matric suction relationship as follows:

$$\frac{\partial \theta_w}{\partial t} = \frac{\partial \theta_w}{\partial \psi} \frac{\partial \psi}{\partial t} = m_w \frac{\partial \psi}{\partial t} = m_w \frac{\partial [(\gamma_w H_w - gy) - P_a]}{\partial t}$$

The time derivative of matric suction will exclude the elevation term above as elevation is constant with time. The air pressure term can be moved to the right side. So the final water flow equation becomes:

$$m_w \gamma_w \frac{\partial H_w}{\partial t} = \frac{\partial}{\partial y} \left[ K_w \frac{\partial H_w}{\partial y} \right] + m_w \frac{\partial P_a}{\partial t} + Q_w$$

where  $Q_w$  has units of length per time.

## Air conservation of mass

Considering the general mass balance equation for air and apply the chain rule to expand the time derivative of the left term:

$$\frac{\partial(\rho_a \theta_a)}{\partial t} = \theta_a \frac{\partial \rho_a}{\partial t} + \rho_a \frac{\partial \theta_a}{\partial t} = \frac{\partial}{\partial y} \left[ (\rho_a K_a) \frac{\partial H_a}{\partial y} \right] + Q_a$$

The time derivative of density can also be expanded using the chain rule and the ideal gas law:

$$\theta_a \frac{\partial \rho_a}{\partial t} = \frac{\theta_a}{RT} \frac{\partial P_a}{\partial t} + \frac{\theta_a P_a}{R} \frac{\partial \left(\frac{1}{T}\right)}{\partial t}$$

where  $R = 287.1 \text{ J/(kg K)}$  for dry air.

The change in air volume over time is the negative of the change in water volume over time and can be related to the change in matric suction:

$$\rho_a \frac{\partial \theta_a}{\partial t} = -\rho_a \frac{\partial \theta_w}{\partial t} = \rho_a m_w \frac{\partial \psi}{\partial t}$$

Combining the previous two equations into the general air flow equation results in:

$$\frac{\theta_a}{RT} \frac{\partial P_a}{\partial t} + \frac{\theta_a P_a}{R} \frac{\partial \left(\frac{1}{T}\right)}{\partial t} + \rho_a m_w \frac{\partial \psi}{\partial t} = \frac{\partial}{\partial y} \left[ \rho_a K_a \frac{\partial \left(\frac{P_a + \rho_a y}{\gamma_w \rho_w}\right)}{\partial y} \right]$$

The air source/sink term on the right,  $Q_a$ , has been removed from the model as it is practically difficult to inject a known mass of air into soil.

This equation can be rearranged:

$$\frac{\theta_a}{RT} \frac{\partial P_a}{\partial t} = \frac{\partial}{\partial y} \left[ \frac{\rho_a K_a}{\gamma_w} \frac{\partial P_a}{\partial y} + \frac{\rho_a^2 K_a}{\rho_w} \right] - \frac{\theta_a P_a}{R} \frac{\partial \left(\frac{1}{T}\right)}{\partial t} - \rho_a m_w \frac{\partial \psi}{\partial t}$$

and the change in matric suction term on the right can be expanded into air and water pressures:

$$\frac{\theta_a}{RT} \frac{\partial P_a}{\partial t} = \frac{\partial}{\partial y} \left[ \frac{\rho_a K_a}{\gamma_w} \frac{\partial P_a}{\partial y} + \frac{\rho_a^2 K_a}{\rho_w} \right] - \frac{\theta_a P_a}{R} \frac{\partial \left(\frac{1}{T}\right)}{\partial t} - \rho_a m_w \frac{\partial (P_a - P_w)}{\partial t}$$

The expanded  $P_a$  term on the right can be combined with the  $P_a$  term on the left and the  $P_w$  can be put in terms of hydraulic head:

$$\left( \frac{\theta_a}{RT} + \rho_a m_w \right) \frac{\partial P_a}{\partial t} = \frac{\partial}{\partial y} \left[ \frac{\rho_a K_a}{\gamma_w} \frac{\partial P_a}{\partial y} + \frac{\rho_a^2 K_a}{\rho_w} \right] - \frac{\theta_a P_a}{R} \frac{\partial \left(\frac{1}{T}\right)}{\partial t} + \rho_a \gamma_w m_w \frac{\partial H_w}{\partial t}$$

### Thermal energy balance

Because the air density is a function of temperature (Fig. 1) it is necessary to solve the energy balance equation. The energy balance equation, with phase change in the water phase, is:

$$(\rho_s c_{ps} + L\theta_w) \frac{\partial \theta_w}{\partial t} = \frac{\partial}{\partial y} \left[ K_t \frac{\partial T}{\partial y} \right] + c_{pa} \frac{\partial (\dot{m}_a T)}{\partial y} + \theta_w \rho_w c_{pw} \frac{\partial (v_w T)}{\partial y} + Q$$

### Solution scheme

Now there are two equations and two unknowns, namely total water head,  $H_w$ , and air pressure,  $P_a$ . If the two equations are rearranged to isolate time derivative of the dependent variables on the left side of each equation the following equations are derived for water and air, respectively:

(i) For water 
$$m_w \gamma_w \frac{\partial H_w}{\partial t} = \frac{\partial}{\partial y} \left[ K_w \frac{\partial H_w}{\partial y} \right] + m_w \frac{\partial P_a}{\partial t} + Q_w$$

On the first iteration, the air pressure term is not known. For all other iterations, it can be obtained from the solution at the previous iteration.

(ii) For air

$$\left( \frac{\theta_a}{RT} + \rho_a m_w \right) \frac{\partial P_a}{\partial t} = \frac{\partial}{\partial y} \left[ \frac{\rho_a K_a}{\gamma_w} \frac{\partial P_a}{\partial y} + \frac{\rho_a^2 K_a}{\rho_w} \right] - \left[ \frac{\theta_a P_a}{R} \frac{\partial \left(\frac{1}{T}\right)}{\partial t} \right] + \left[ \rho_a \gamma_w m_w \frac{\partial H_w}{\partial t} \right]$$

The second and third terms on the right side can be explicitly applied as sources or sinks. The third term in the above equation on the right side is known from the previously solved seepage equation at each iteration.

### Air Column

Unfortunately, few data sources are available to validate the model. In order to check the mechanisms, an air column was modeled, testing the gravity driven air convection. Appropriate air thermal properties are chosen (eg. Andersland and Ladanyi, 2004) and the air permeability is set to 500m/day. The initial temperature of a 5m height column is 0°C. The surface temperature was reduced to -8°C within 7.5 days before it was sinusoidal altered between -8°C and +5°C within 15 days for a total duration of 112.5 days, ie. 3.75 cycles. Figure 2 shows the differences between the convective and the conductive model for the last stages with minimum and maximum temperature at the top. The pure conduction model shows less change in the temperature gradient with depth. The model that considers gravity driven air movements, on the other, shows a cooling trend for deeper layers at both time steps. This effect can clearly be attributed to the sinking of dense and cold air.

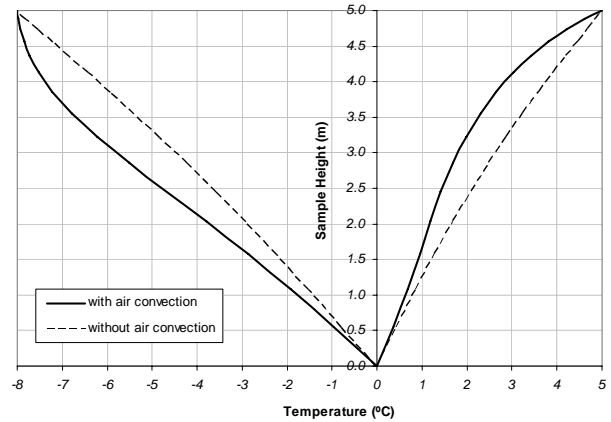


Figure 2. Comparison of temperatures within an air column with and without convective air flow.

These results clearly demonstrate that the new numerical code is capable of modeling the physical processes that are observed in nature.

### Road Embankment

Ciro and Alfaro (2005) presented the effect of global warming on the ground thermal regime beneath a road embankment. They use the climate model CGCM2, scenario A2 (Flato et al., 2000; Flato and Boer, 2001; CCCma, 2006) to reproduce the future air temperatures. The model was run for 50 years. Significant warming of the ground and permafrost degradation below the embankment was predicted with a complete thawed section underneath the embankment after 20 years. Such a large change in the ground temperatures most probably will result in major

damages to the road and require considerable maintenance costs.

The numerical model used is exclusively based on conductive heat fluxes. In addition, changes in thermal properties of the peat layer as a function of thaw consolidation were ignored.

## Improved Road Embankment Design

### Material Properties

The material properties used for the new model are based on the properties presented by Ciro and Alfaro (2005). Their example was used to demonstrate the changes in the ground temperatures as an effect of air convection. The material properties used are summarized in Table 1.

Table 1. Material properties.

Material	Thermal properties			
	Thermal conductivity <i>kJ/(day·m·K)</i>		Volumetric heat capacity <i>kJ/(m<sup>3</sup>·K)</i>	
	frozen	unfrozen	frozen	unfrozen
Embankment	346	242	3380	4118
Peat	91	36	2452	4328
Clay	173	138	2920	4174
Protection	190	190	2000	2000

Material	Mechanical properties		
	vol. water content, saturated	sat. hydraulic permeability	dry air permeability
Embankment	0.14%	10 <sup>-2</sup> m/s	0.01m/h
Peat	0.89%	10 <sup>-6</sup> m/s	0.01m/h
Clay	0.33%	10 <sup>-10</sup> m/s	0.01m/h
Protection	0.05%	-	variable

### Air Temperatures

In contrast to Ciro and Alfaro (2005), air temperatures were simplified by using a sinusoidal distribution, which, however, had similar mean annual air temperatures (MAAT) as well as freezing and thawing days. The n-factors are very important for the modeling of the ground thermal regimes and even small changes can have significant influences on the ground temperatures. For the protection, a value close to 1 was chosen indicating that the ground surface temperatures are close to the air temperatures. In order for the protection to work properly insulating effects from thick snow covers during winter have to be reduced. The remaining n-factors were chosen as suggested by the authors of the original model (Tab. 2).

The effect of warming was simply analyzed by increasing the MAAT by 1.35°C, mainly due to warming during the winter (Fig. 3). The air freezing index increased from 3635 °C·day to 3143 °C·day, and the air thawing index decreased from 1564 °C·day to 1558 °C·day, respectively.

Table 2. n-factors for the surface of the model.

Surface	freezing n-factor	thawing n-factor
Asphalt	0.9	1.9
Slope	0.3	1.5
Peat	0.3	0.73
Protection	0.8	1.2

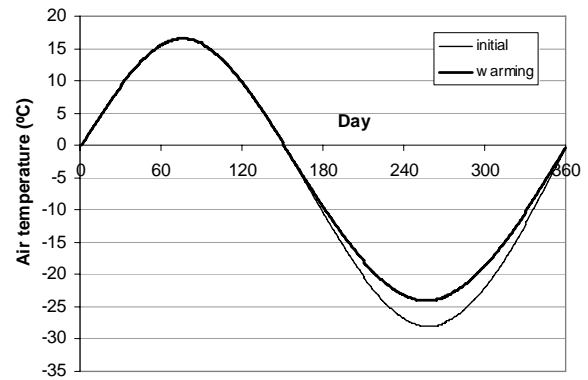


Figure 4. Air temperature distribution.

### Numerical Modeling

Not only was the air temperature variation simplified, but also the geometry of the embankment (Fig. 4). Similar temperature distributions were obtained by ignoring convective heat fluxes and the existence of the protection.

The embankment design was changed after the initial conditions were established and a high air permeable protective layer was added on the side slope. Three different designs for the protection were investigated (Fig. 5).

The air flow within this layer cools the ground below and reduces permafrost degradation. In order to study the effect of air permeability in the protective zone, this value was varied between 1m/h and 100m/h. Figure 6 shows the temperatures in the protective layer type II after one year, ie. one warming and one cooling cycle. An increase in air permeability results in a cooling effect within the core of the protection. In addition, the cold air sinks cooling the ground below the protection.

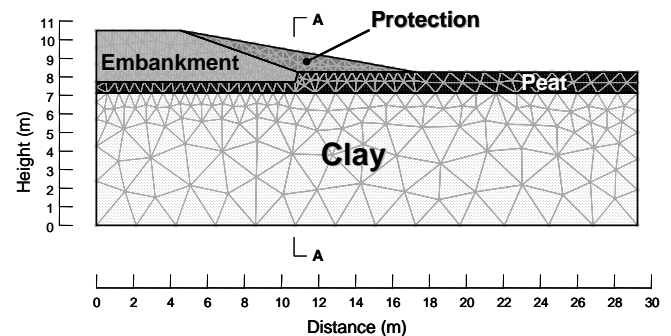


Figure 4. Embankment geometry and mesh.

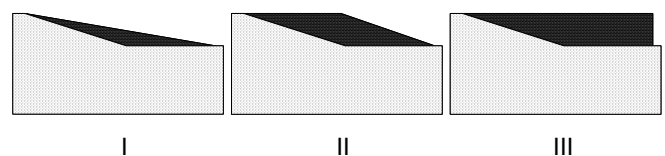


Figure 5. Different protection geometries.

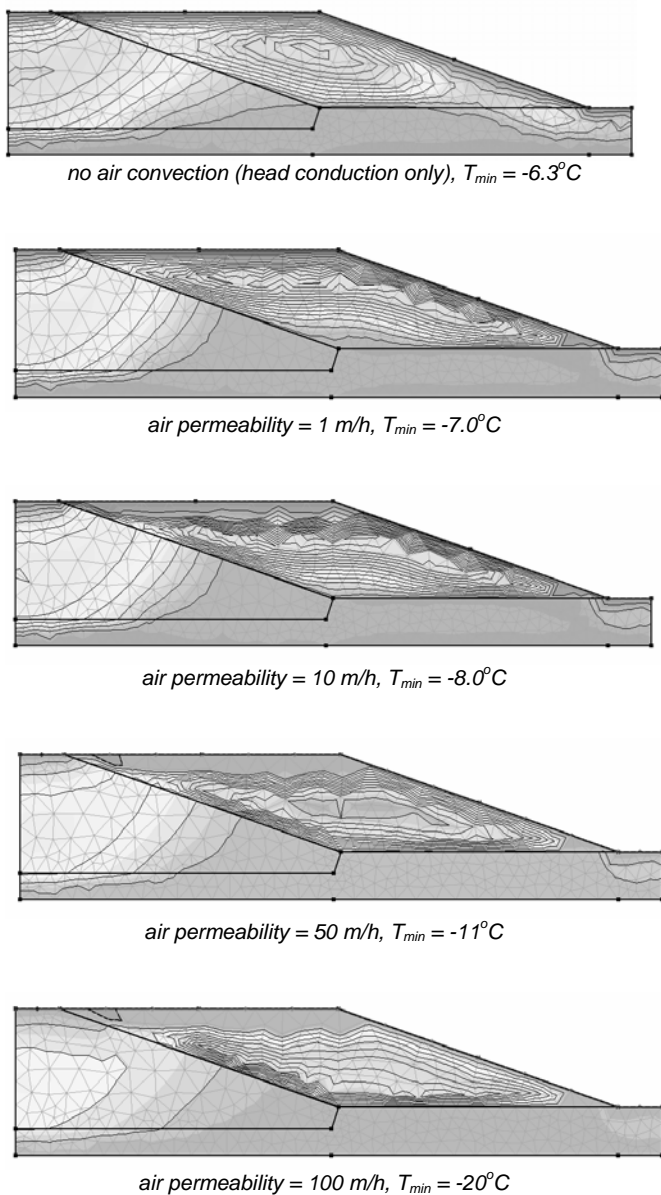


Figure 6. Temperatures in the protective layer type II after one year for conduction only and different air permeabilities.

The cooling effect is mainly controlled by the amount of air that flows through the protection layer. In addition, the heavy air has to remain within the protective layer, which requires some sort of cover at the bottom or the lower part of the protection. Depending on the cooling effect required, different material properties have to be chosen that allow for the necessary air permeability. Based on the initial trials, protection type II was used with an air permeability of 10m/h to model the long term effect on the embankment.

The boundary conditions at the surface of the protection were assigned so that air can enter at the top of the protection, but only exit close to the toe. This configuration guaranteed an air movement through the protection as well as that the cold air stayed within, producing the required cooling effect.

Figures 7, 8 and 9 show the ground temperature distributions within the ground for different scenarios, stages and depths. A cooling effect can be noted under the embankment. Without the protection, the permafrost within the clay layer had degraded within the modeled period of five years. The protection manages to maintain the temperatures below zero centigrade for a longer time. However, after four years the situation below the embankment is again very critical. It has to be noted that the scenario used is very problematic for the temperature conditions selected since the ground temperatures for the initial stage are very close to zero degree. The most important effect the protection generates is a cooling below the centre of the embankment. The warming of the ground is shifted towards the open field, ie. the right for the configuration shown. This shift reduces the sensitivity of the ground directly below the embankment and less settlement is expected. The rise in the zero degree isotherm is reduced significantly by including the air convection (Fig. 8).

Below the toe of the initial embankment the temperatures rise very quickly when convection is ignored (Fig. 9). The model showed that for these circumstances permafrost degradation can not be avoided completely, but the process can be slowed significantly. After one year, some cooling could be achieved with the protection at lower depth, mainly because of the cold buffer that develops in the protection. However, the severe warming manages to overcome some of this beneficial effect and start warming the ground at greater depths as well.

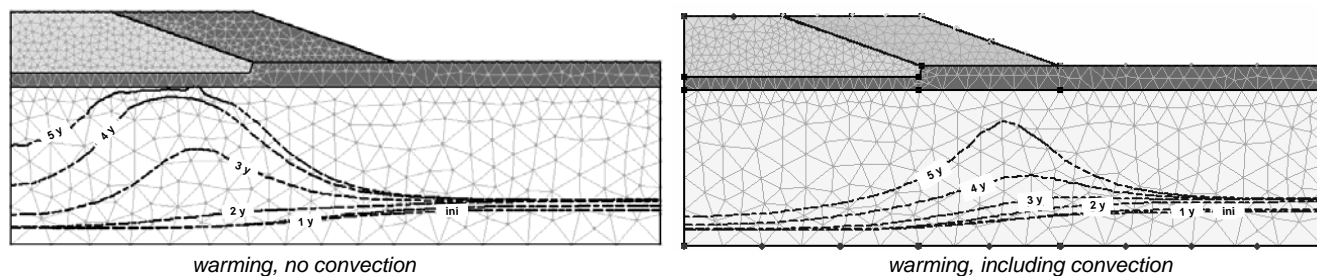


Figure 7. Change in zero degree isotherm over five years for warming with and without convection.

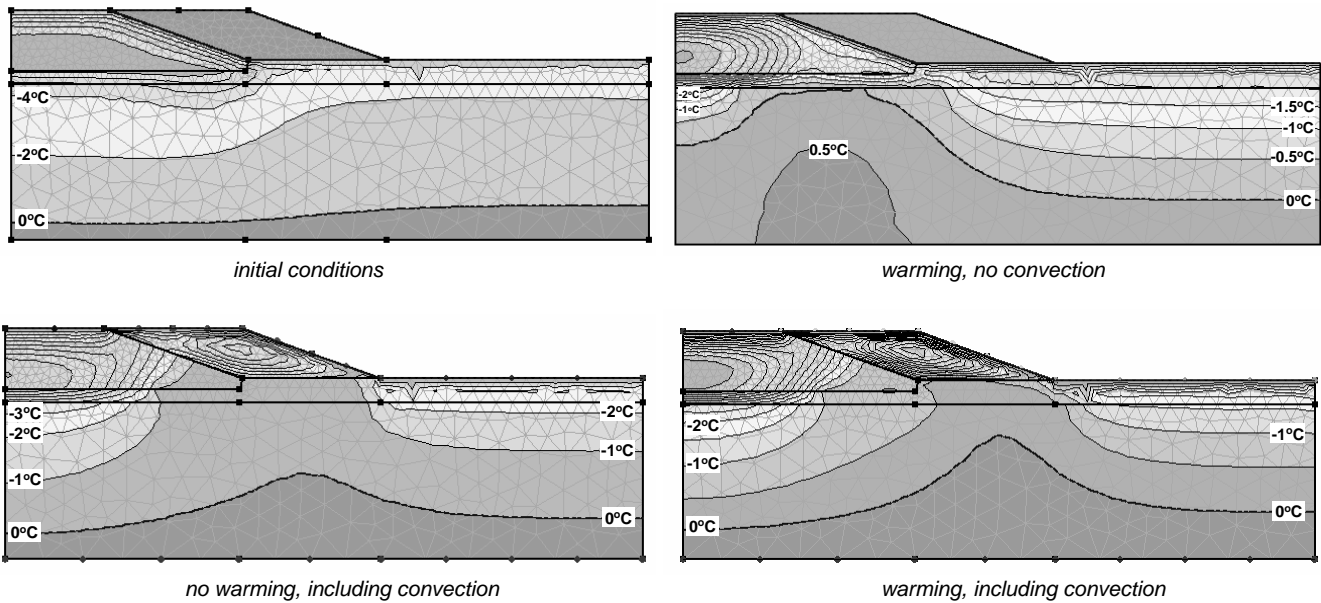


Figure 8. Initial ground temperature conditions and temperatures after five years with and without protection.

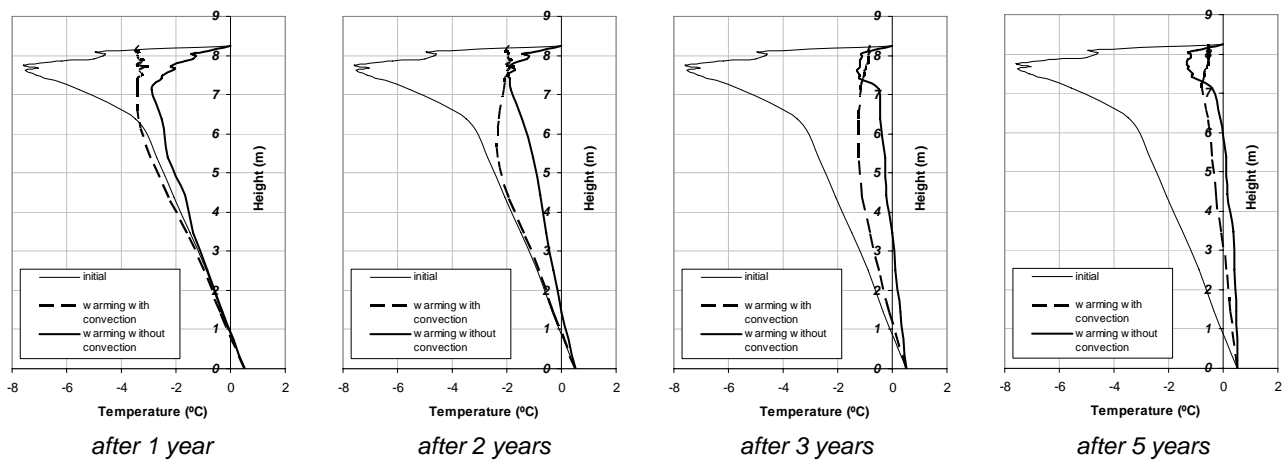


Figure 9. Temperature profiles with depth in section A-A for different time steps.

## Discussion

The new numerical code allows for studying the effect of air convection on the ground thermal regime, in particular, where gravity driven air movements play an important role. Initial simulations have demonstrated that existing embankments can be improved by adding a protective layer on the side slopes that forces cold air to penetrate during the cold winter months and acting as insulation during warmer summer months. The air permeability of the layer as well as the cover properties influence the efficiency of the air convection.

It is important that the cold air can penetrate into the protective layer and stay during the warm summer months. In addition, the air permeability has to be high enough so that the gravity driven effect can develop. Despite the physical properties, such as air permeability and the thermal properties, additional aspects have to be

considered. Even though design type III might give the best protection, it is not suitable for highways, where cars may drive off the road. A reduction in the side slope angle, type I, might improve road safety as well as foundation conditions. It is, however, important that air can enter the layer at the desired location, ie. coarse material has to be used at the surface.

In order to guarantee high air permeability and optimal insulating effects, very coarse rocks have to be used and clogging has to be avoided. In addition to the high air permeability, light weight concrete can also significantly reduce the thermal conductivity of the protection, furthering the beneficial effect of the air convection.

In addition to the thermal properties, n-factors, ie. penetration of air temperatures into the ground, have to be considered. For the system to work it is important to

protect the slopes from intense warming during summer and from insulating during winter by a thick snow cover.

One of the biggest challenges with numerical modeling ground temperature changes due to air convection is the determination of the ratio between the air conductivity, the time steps and the mesh spacing. If these three factors are not in balance with each other, numerical instabilities or incorrect results have to be expected, in particular for high air pressure gradients. Depending on the boundary conditions, maximum time steps may have to be smaller than one minute, which requires significant CPU time to model large problems. However, the optimal ratios are not yet evaluated and are subject of current modeling efforts. In order to keep computational times within a reasonable range, a situation was modeled, for which degradation were to observe within the next decade even without any change in air temperature. The extreme circumstances chosen allowed for demonstrating the beneficial effect of air convection using one particular protection design.

The validation of the program is difficult due to the limited amount of data available that record heat convection within an embankment. However, an initial comparison using the new code to model air convection in a test embankment (Saboundjian and Goering, 2003) is showing promising results (Klassen et al., 2006).

## Conclusions

Convective heat fluxes can have a significant influence on ground thermal regimes. A new numerical model that allows for modeling temperature induced convective heat flow was used to propose possible designs to protect embankment foundations in warm permafrost regions from degradation and hence substantial maintenance costs. The measures proposed are simple to be put in place and more economical than complete new road designs and construction. In addition, it is expected that the life-span of the road can be extended.

It is important to note that the actual design and material used has to be adjusted to a particular location, subsurface condition as well as predicted local climatic change. An improvement technique such as the one presented in this paper is very flexible and changes can be made to the design in the future as improved temperature forecasts, effectiveness of different designs, or improved material parameters are available. In such a way the ground thermal behavior may be influenced relatively accurate.

As shown amongst others by Ma (2006), using air convection in the design of an embankment helps to keep the ground from thawing. The physical processes involved are quite complex and depend on a number of factors, such as the air permeability, water content, or air boundary conditions. Numerical models help in understanding and quantifying these processes and influences. However, field data are required to calibrate the new numerical models. In addition to ground temperatures, air velocities have to be measured to determine the ground air permeability. Based on these data, designs for the protection of the permafrost due to infrastructures can be further optimized and mitigation strategies can be prepared.

## Acknowledgement

The first author thanks the Swiss National Science Foundation (grant No PA002-108947) for the financial support.

## References

- Andersland, O.B., and B. Ladanyi. *An introduction to frozen ground engineering*, 2004.
- CCCma. Canadian Centre for Climate Modelling and Analysis, 2006.
- Cheng, G.D. A roadbed cooling approach for the construction of Qinghai-Tibet Railway. *Cold Regions Science and Technology*, 42 (2): 169-176, 2005.
- Ciro, G.A., and M.C. Alfaro. Modeling of ground thermal regime in degrading permafrost beneath road embankments. *Proceedings, 58th Canadian Geotechnical Conference*, Saskatoon, SK, Canada: CD-Rom, 2005.
- Flato, G.M., and G.J. Boer. Warming asymmetry in climate change simulations. *Geophysical Research Letters*, 28 (1): 195-198, 2001.
- Flato, G.M., G.J. Boer, W.G. Lee, N.A. McFarlane, D. Ramsden, M.C. Reader, and A.J. Weaver. The Canadian centre for climate modelling and analysis global coupled model and its climate. *Climate Dynamics*, 16 (6): 451-467, 2000.
- Goering, D.J., and P. Kumar. Winter-time convection in open-graded embankments. *Cold Regions Science and Technology*, 24 (1): 57-74, 1996.
- Instones, A. Infrastructure: buildings, support systems, and industrial facilities. *Arctic Climate Impact Assessment 2005*, Cambridge University Press: 907-944, 2005
- Kane, D.L., K.M. Hinkel, D.J. Goering, L.D. Hinzman, and S.I. Outcalt. Non-conductive heat transfer associated with frozen soils. *Global and Planetary Change*, 29 (3-4): 275-292, 2001.
- Klassen, R., L.U. Arenson, and D.C. Sego. Heat convection modeling in embankments. *Proceedings, 59th Canadian Geotechnical Conference*, Vancouver, BC, Canada: (in preparation), 2006.
- Lai, Y.M., Q.S. Wang, F.J. Niu, and K.H. Zhang. Three-dimensional nonlinear analysis for temperature characteristic of ventilated embankment in permafrost regions. *Cold Regions Science and Technology*, 38 (2-3): 165-184, 2004a.
- Lai, Y.M., S.J. Zhang, L.X. Zhang, and J.Z. Xiao. Adjusting temperature distribution under the south and north slopes of embankment in permafrost regions by the ripped-rock revetment. *Cold Regions Science and Technology*, 39 (1): 67-79, 2004b.
- Liu, Z.Q., and Y.M. Lai. Numerical analysis for the ventilated embankment with thermal insulation layer in Qing-Tibetan railway. *Cold Regions Science and Technology*, 42 (3): 177-184, 2005.
- Ma, W., C.-h. Shi, Q.-b. Wu, L.-x. Zhang, and Z.-j. Wu. Monitoring study on technology of the cooling roadbed in permafrost region of Qinghai-Tibet plateau. *Cold Regions Science and Technology*, 44 (1): 1-11, 2006.
- Saboundjian, S., and D.J. Goering. Air convection embankment for roadways - Field experimental study in Alaska. *Geology and Properties of Earth Materials 2003, Transportation Research Board, National Research Council*, Washington, DC: 20-28, 2003

- Smith, S.L., and M.M. Burgess. Mapping the response of permafrost in Canada to climate warming. *Current Research 1998-E*, Geological Survey of Canada, 1998.
- Smith, S.L., and M.M. Burgess. Mapping the sensitivity of Canadian permafrost to climate warming. *Interactions between the cryosphere, climate and greenhouse gases (Proceedings of IUGG 99 Symposium HS2)*, Birmingham, UK: 71-80, 1999.
- Wu, Q.B., Y.Z. Liu, J.M. Zhang, and C.J. Tong. A review of recent frozen soil engineering in permafrost regions along Qinghai-Tibet Highway, China. *Permafrost and Periglacial Processes*, 13 (3): 199-205, 2002.
- Yu, Q.H., C.H. Shi, F.J. Niu, N.W. He, and K. Roth. Analysis of temperature controlled ventilated embankment. *Cold Regions Science and Technology*, 42 (1): 17-24, 2005.

## Symbols

$H$	total energy potential
$K$	permeability
$L$	latent heat of water
$P$	pressure
$Q$	external energy flux (source/sink)
$R$	gas constant for air = 287.1 J/(kg·K)
$T$	absolute temperature
$m_v$	slope of the water content versus matric suction relationship
$\rho$	density
$\theta$	volume
$\psi$	matric suction
$v$	specific discharge (Darcy velocity)
$\rho_s c_{ps}$	volumetric heat capacity of soil
$c_{pa/w}$	mass specific heat of air or water
$\dot{m}_{a/w}$	mass flow rate of air
$\frac{\partial \theta_u}{\partial T}$	slope of the unfrozen water content function

### Subscripts:

$a$	air
$f$	fluid
$w$	water